C – Test Cases

Note: The files corresponding to the following test cases are supplied with the software.

C1 – Laminar Flow between Two Parallel Plates

File: LaminarProfile.def

The analytical solution for the developed laminar flow between two parallel plates is given by:

$$V = -\frac{1}{2\mu}\frac{dp}{dx}\left(H^2 - z^2\right) \tag{1.1}$$

where H is half the distance between the plates and z is the coordinate normal to the plates, starting at the symmetry plane (cf. Figure C.1(a)). The longitudinal pressure gradient is:

$$\frac{dp}{dx} = -\frac{3\overline{V}}{H^2}\mu \tag{1.2}$$

where $\overline{V}$ is the average velocity. The maximum velocity, reached at the symmetry plane ($z=0$), may be obtained by substituting equation (1.2) into (1.1):

$$V_{max} = 1.5\overline{V}$$

Computations were carried out in half the domain, imposing a symmetry boundary condition and using a uniform grid spacing (Figure C.1). To obtain a developed velocity profile without using a very large length, the option *Profile* was activated when imposing the inlet boundary condition (cf. section B1.6.2).

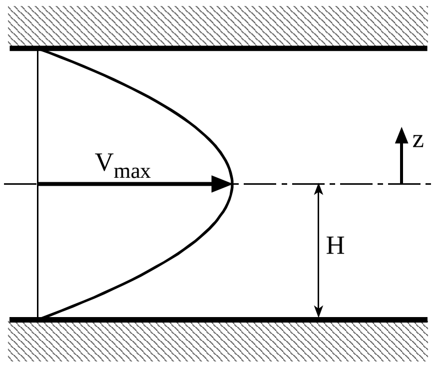

(a)

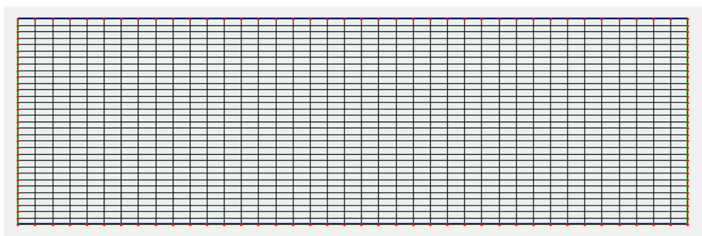

(b)

Figure C.1 – Problem definition. (a) schematic drawing; (b) EasyCFD calculation domain.

Figure C1.1 – Problem definition.

The following values where used:

$H = 0.04\,m$; $\overline{V} = 10^{-3}\,m/s$; fluid: water ($\mu = 10^{-3}\,N\,s/m^2$; $\rho = 10^3\,kg/m^3$)

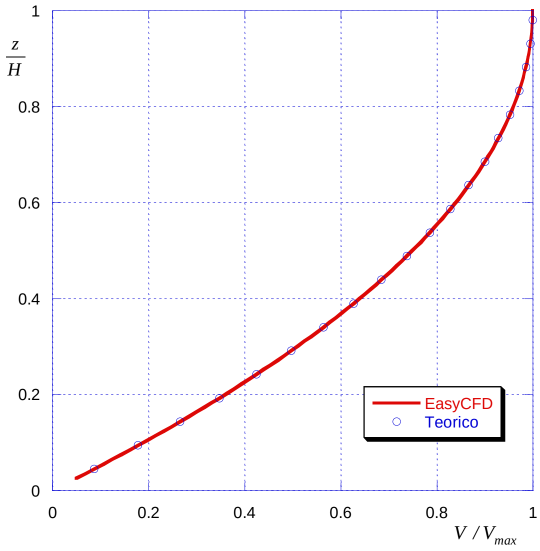

Figure C.2 – Velocity profile.

Figure C.2 shows the obtained velocity profile overimposed on the theoretical solution. As one may observe, the two curves are practically coincident. For this case, the theoretical pressure gradient is:

$$\left(\frac{dp}{dx}\right)_{theoretical} = -\frac{3\times10^{-3}}{0.04^2}\times10^{-3} = 1.875\times10^{-3}\,Pa/m$$

To compute the pressure gradient given by the **EASYCFD** results, the *Export* feature was used to open an Excel sheet for pressure along an horizontal line (cf. section B3.9.1). The obtained value is:

$$\left(\frac{dp}{dx}\right)_{EasyCFD} = 1.8736\times10^{-3}\,Pa/m$$

The maximum velocity, at the symmetry plane, given by the software, is $V_{max} = 1.497\,m/s$, while the theoretical value is *1.5 m/s*.

As a suggestion, you certainly may improve these results by using a more refined grid with a better clustering near the low boundary.

C2 – Turbulent Flow between Two Parallel Plates

File: TurbulentProfile.def

As for the previous case, computations where performed in half the domain, imposing a symmetry boundary condition. In order to resolve the flow near the wall, proper clustering was ensured at this boundary (cf. Figure C.3). To obtain a developed velocity profile without using a very large length, the option *Profile* was activated when imposing the inlet boundary condition (cf. section B1.6.2).

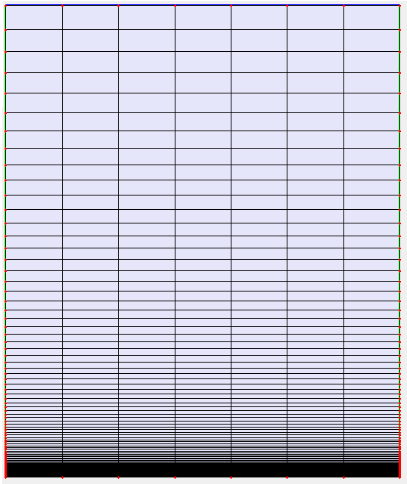

Figure C.3 – Mesh used.

According to the following values adopted for this problem,

$H = 0.6\,m$; $\overline{V} = 1\,m/s$; fluid: air ($\mu = 1.824\times10^{-5}\,N\,s/m^2$; $\rho = 1.1884\,kg/m^3$)

the flow Reynolds number is 39092. Computations where carried out using the *SST k-ω* turbulence model. Due to its hybrid characteristics, unlike the standard *k-ε* model, this model allows computations to be done in the viscous sublayer.

The obtained results were compared with the direct numerical simulation presented by Kim et al., 1987, which were done for a Reynolds number of 3300. Figure C.4 displays the boundary layer profile obtained with both simulations. Note that, due to the lower Reynolds number adopted by Kim et. al., their range of u^+ values is not as large as the present one. One may note a very good agreement, except for the transition between the viscous and the log layer.

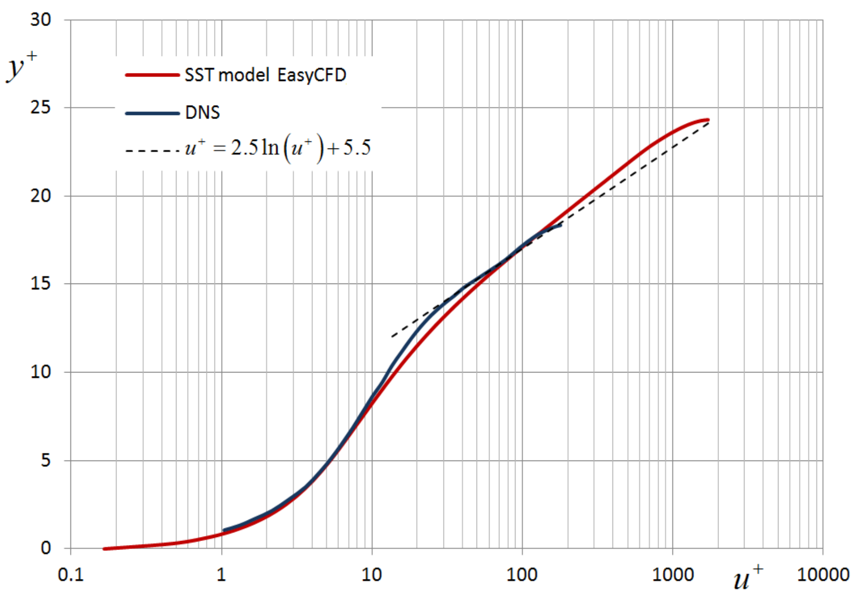

Figure C.4 – Boundary layer profile.

C3 – Turbulent Flow Over a Backward-Facing Step

File: Step.def

The flow over a backward-facing step (Figure C.5) is a typical problem for the validation of turbulence models and their implementation. This is a rather simple geometry, where the flow separation point is fixed at the step corner. The reattachment length depends on the Reynolds number and on the ratio between the inlet and the outlet sections. The prediction of the reattachment position is a demanding test for the turbulence model, as it is quite sensitive to the fluid effective viscosity.

In the present case, the flow Reynolds number, based on the inlet centreline velocity and on the height of the outlet section, is *132000*. Present results are compared with the ones described by Ting and Prakash (2005) and by Papageorgakis and Assanis (1999). The first work presents, among others, (1) results obtained with the k-ε model in a version implemented in the commercial software Fluent, using wall laws; (2) computations performed by Thangam and Hur (1991) with the k-ε model and (3) experimental results obtained by Kim et al. (1978). In these works, authors took, for the inlet boundary, a previously developed velocity profile. Papageorgakis and Assanis (1999) show calculations obtained with the *RNG* linear and the non-linear k-ε model, for $Re=135000$.

The hybrid discretisation scheme and the harmonic interpolation for viscosity were adopted. The grid has 179×102 nodes, with *15807* active nodes

In the present case, the inlet velocity profile was obtained with the feature *Profile* activated. Figure C.6 presents the inlet velocity profile thus obtained, along with the profile by Ting and Prakash (Fluent code) and by Papageorgakis and Assanis. As one may observe, the developed profile agrees well with the experimental data (another possible approach would be to use a *TableFunction* to assign the inlet profile according to the experiments).

Figure C.7 displays the streamlines in the recirculation region downstream of the step, together with the results computed by other authors. The reattachment point was calculated, by **EasyCFD**, at $x/H=6.4$, while Ting and Prakash present the values *6.28*, *6.30* and *5.7* for other works. Papageorgakis and Assanis refer values in the range of *7.35* to *8.3*.

The graphics in Figure C.8 represent the velocity profile at different locations downstream of the step. The differences between the several contributions are certainly also due to the different inlet velocity profiles. The predictions of both Fluent and **EasyCFD** underestimate the length of the recirculation region, a well known characteristic of the predictions given by the k-ε model for this type of flows.

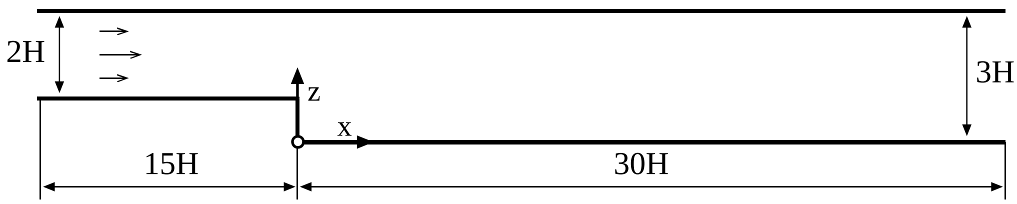

Figure C.5 – Geometrical configuration of the backward facing step (the drawing is not to scale).

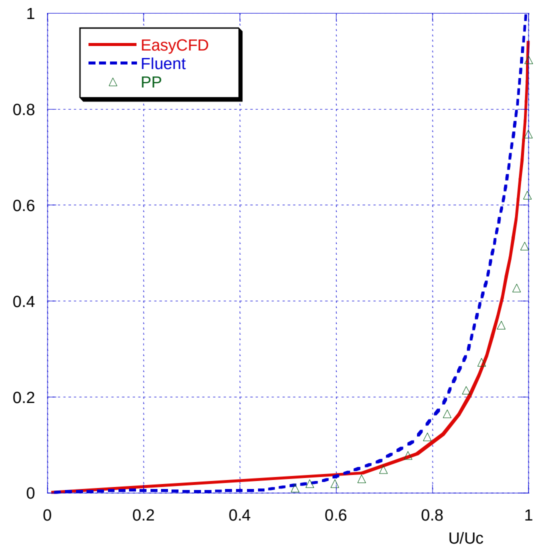

Figure C.6 – Inlet velocity profile.

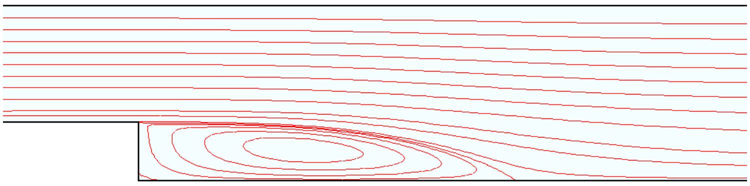

(a) – EasyCFD

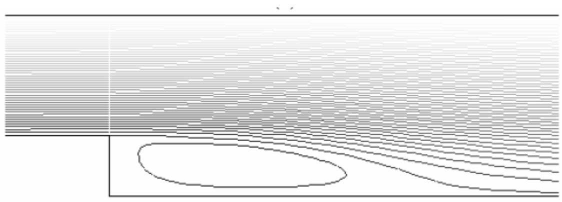

(b) - Fluent (in Ting and Prakash 2005)

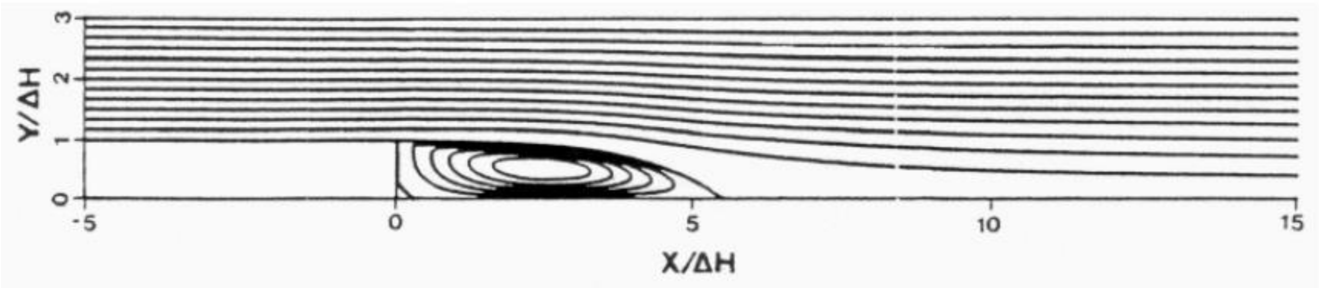

(c) - Thangam and Hur (1991)

Figure C.7 – Streamlines in the recirculation region.

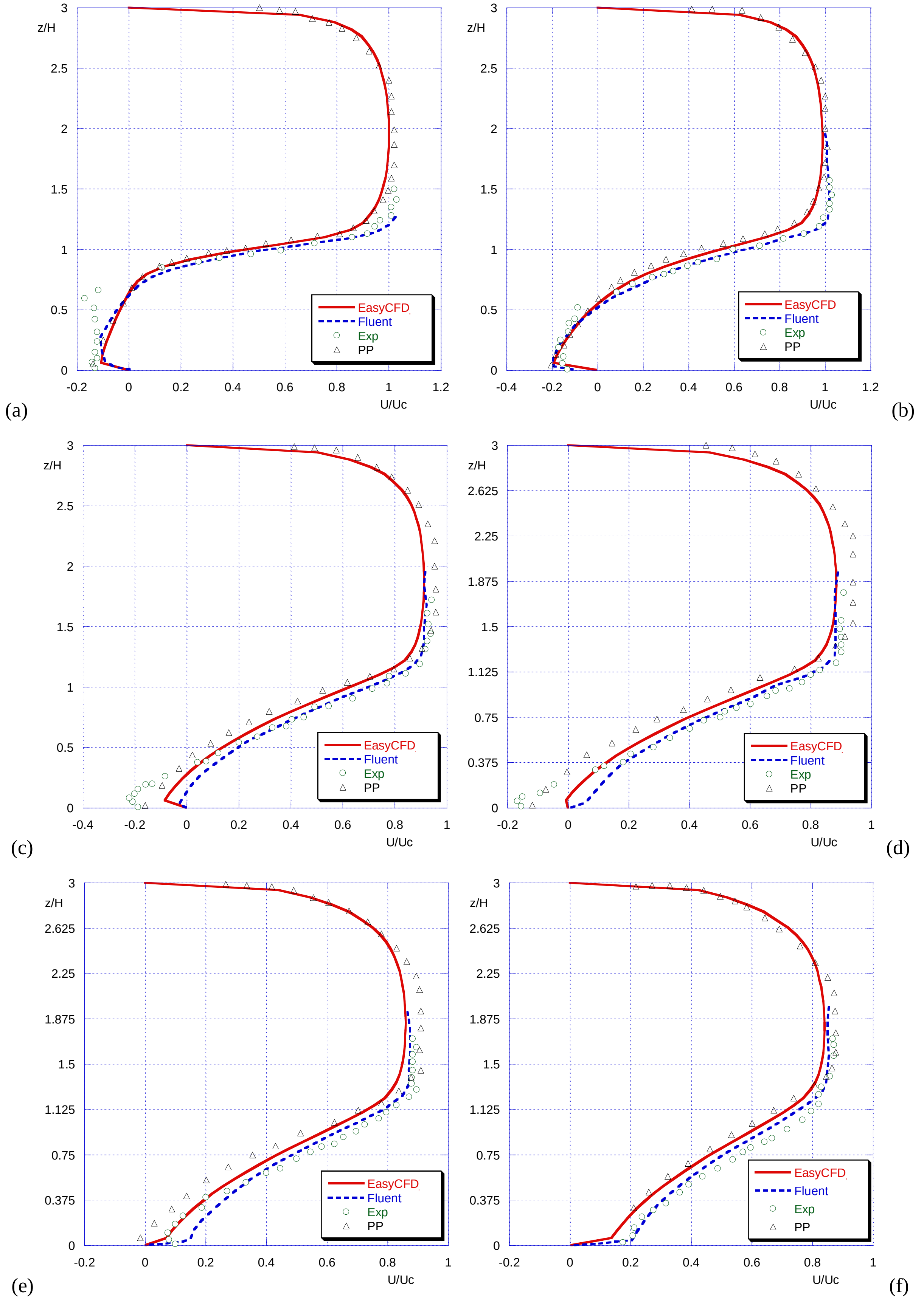

Figure C.8 – Velocity profiles several locations downstream of the step.

(a) - x/H=1.333; (b) - x/H=2.667; (c) - x/H=5.333; (d) - x/H=6.220; (e) - x/H=7.113; (f) - x/H=8.0

C4 – Natural Convection Inside a Cavity

File: ConvLam.def

The natural convection flow in a cavity is a classical test for the numerical methods in fluid dynamics. In this problem, constant temperature is imposed in two vertical walls. The horizontal walls are adiabatic (cf. Figure C.9).

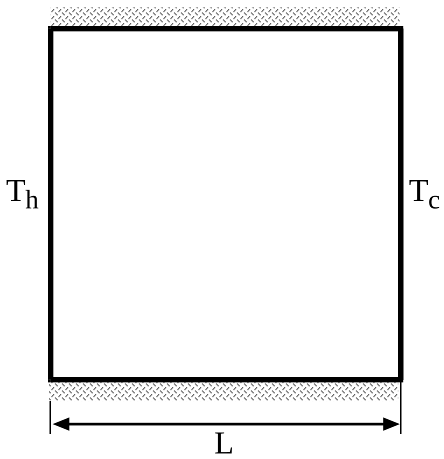

Figure C.9 – Problem definition.

The problem is governed by the following non-dimensional parameters:

$$\text{Prandtl number, } Pr = \frac{\nu}{\alpha}$$

where the thermal diffusivity is $\alpha = \lambda / \left(\rho c_p\right)$, ν is the kinematic viscosity, λ is the thermal conductivity, ρ is the density and c_p is the heat capacity.

$$\text{Rayleigh number, } Ra = \frac{g\,\beta\,\Delta T\,L^3\,Pr}{\nu^2}$$

where β is the thermal expansion coefficient, g is the gravity acceleration and $\Delta T = T_h - T_c$ is the temperature difference between the vertical walls.

The transition between laminar and turbulent flow takes place for $Ra = 10^7$, approximately. Results are present Rayleigh number $Ra = 10^5$ (laminar regime). Air is the operating fluid, for which $Pr = 0.71$.The hybrid advection scheme was used and the Boussinesq approximation was adopted.

Computations were performed in a non-uniform grid, with $82 \times 82 = 6400$ nodes. Vahl Davis (1983) and Vahl Davis et al. (1983) report reference results for several Rayleigh numbers in laminar regime and compare solutions given by several authors. Dixit and Babu (2006) present results for laminar and turbulent flow.

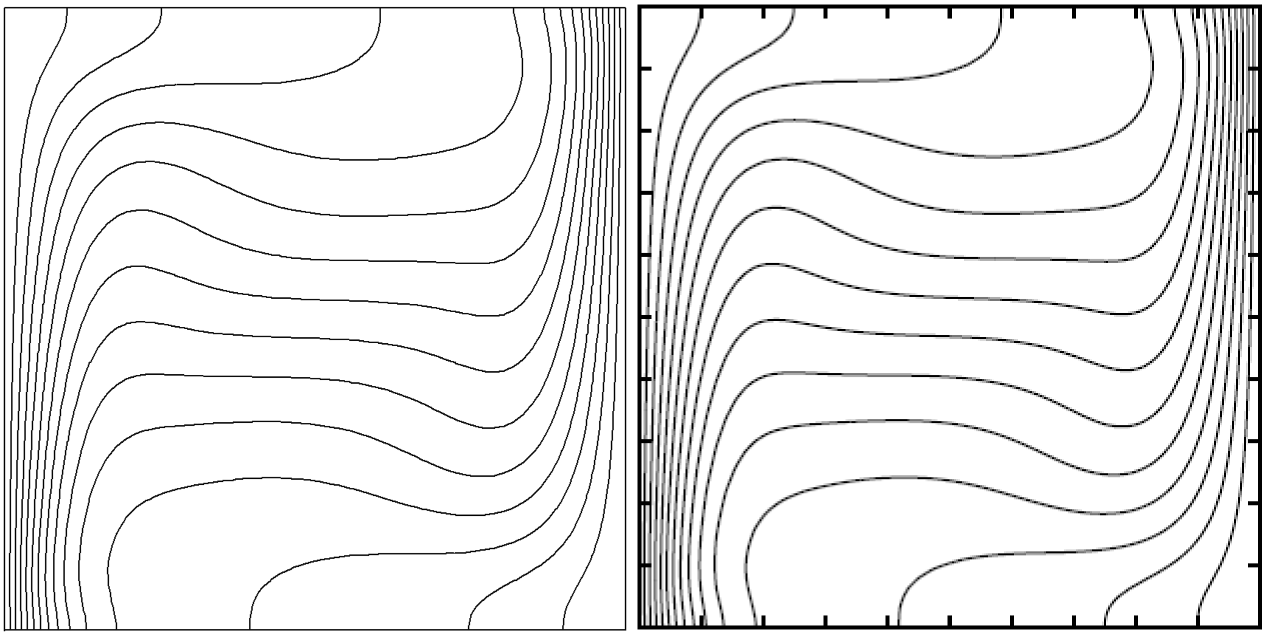

(a) – EasyCFD (b) – Dixit and Babu (2006)

Figure C.10 – Isothermal lines. $Ra=10^5$.

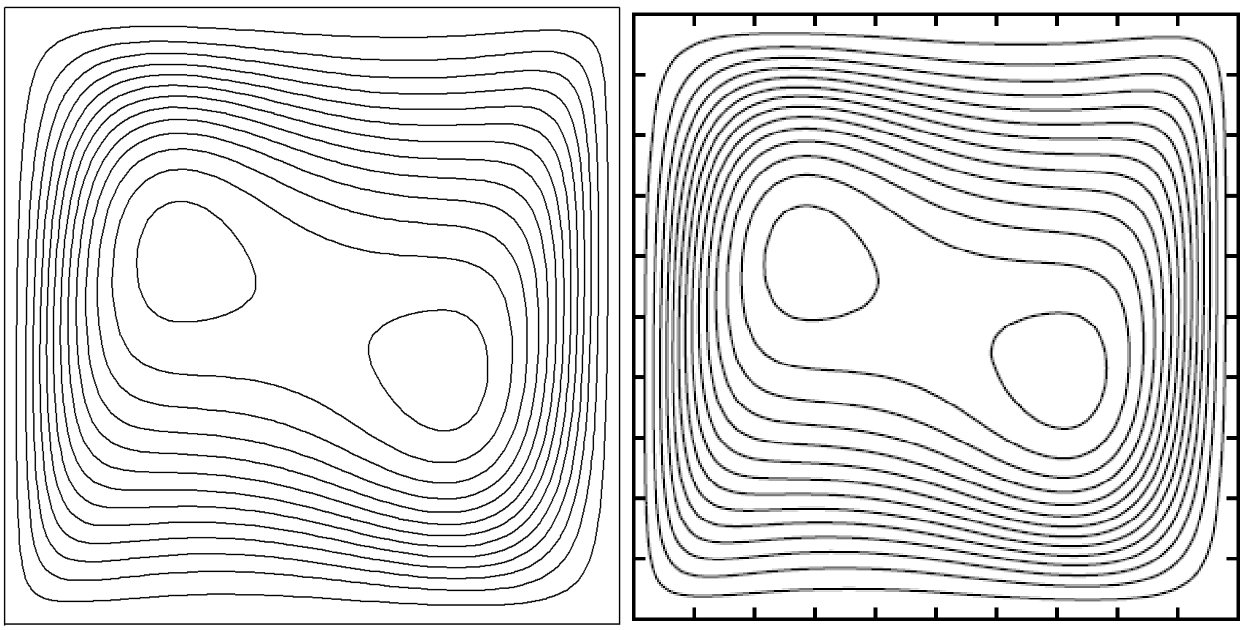

(a) – EasyCFD (b) – Dixit and Babu (2006)

Figure C.11 – Streamlines. $Ra=10^5$

Figure C.10(a) and (b) display the isothermal lines, generated using uniform value spacing between the minimum and the maximum verified within the domain. Figure C.11(a) and (b) represent the flow streamlines. For this case, the minimum and the maximum values used do not correspond to the amplitude of the stream function within the domain. These values were adjusted in **EasyCFD** to correspond to those employed in Dixit and Babu (2006). The agreement between the calculations is quite good, for both types of results.

Vahl Davis and Jones (1983) present normalised maximum values for the *u* and for the *w* components of velocity:

$$u^* = \frac{u\,L}{\alpha} \quad ; \quad w^* = \frac{w\,L}{\alpha}$$

occurring in the vertical and in the horizontal symmetry plane, respectively. Table 2 shows the results obtained with **EasyCFD**, the reference values of Vahl Davis and the range of variation for the *37* contributions reported by Vahl Davis and Jones (1983). This range does not include the minimum and the maximum reported values, since these clearly fall outside the general trend of the remaining contributions.

Table 2

	EasyCFD	Vahl Davis	Interval
u^*_{max}	*34.44*	*34.81*	*34.2-41.2*
w^*_{max}	*68.21*	*68.68*	*65.8-70.45*

C5 – Pulsatile Flow Inside a Symmetric Channel with Wavy Walls

File: PulsatileFlow.def

This problem concerns a pulsatile laminar flow inside a channel symmetric with sinusoidal walls. The geometrical configuration is presented in Figure C.12.

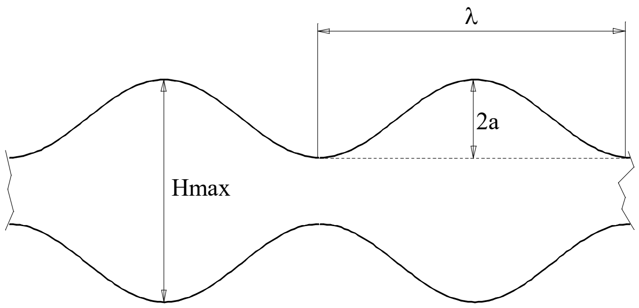

Figure C.12 – Geometry for the wavy channel.

The instantaneous inlet flow is defined by:

$$Re_i(t) = Re_m\left(1 + A\sin\left(2\pi t / T\right)\right)$$

where t is time, T is the oscillation period, A is the oscilation amplitude and Re_m is the average Reynolds number:

$$Re_m = \frac{Q_m}{\nu}$$

with Q_m as the volumetric flowrate per unit depth.

The temporal scale is given by the Womersley number, α^2:

$$\alpha^2 = \frac{H_{max}^2 2\pi / T}{\nu}$$

The dimensionless time t* is defined as:

$$t^* = \frac{t}{T}$$

For the present case, the following values where considered:

Geometrical parameters: $2a = 3.5mm$ $H_{max} = 10mm$ $\lambda = 14mm$

Flow parameters: $\alpha^2 = 650$ $A = 2.5$ $Re_m = 50$

Figure displays the instantaneous Reynolds number as function of the dimensionless time, for an entire cycle.

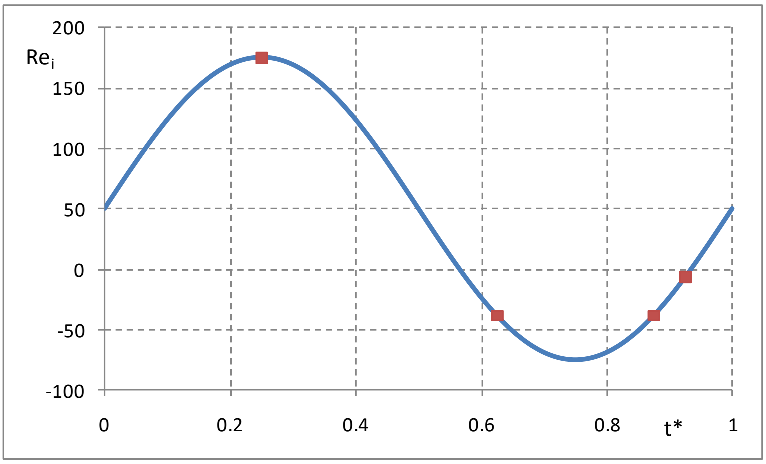

Figure C.13 – Instantaneous Reynolds number as function of the dimensionless time. Red dots represent time instants for Figure C.15.

The channel is periodic. In the present implementation, 3 waves were considered, and periodic boundary conditions were implemented by using the *Profile* option for the inlets (cf. Figure C.14). The velocity value is imposed at the two inlets, using *TableFunctions* with opposite sign as function of time (thus, at a certain time instant, there will be one inlet and one outlet). Although two entire temporal cycles were simulated (in order to achieve a developed flow in temporal terms), only one cycled needs to be specified in the *TableFunction*; since the first and the last velocity values are similar, periodic conditions are automatically assumed. Comparison with data by Nishimura and Matsune (1998) is presented in Figure C.15, at the central wave, for different values of the adimensional time $t*$ (cf. red dots in Figure C.13; the streamlines values used in the comparison is not the same, as these authors don´t mention the criterion followed for the choice of the streamlines).

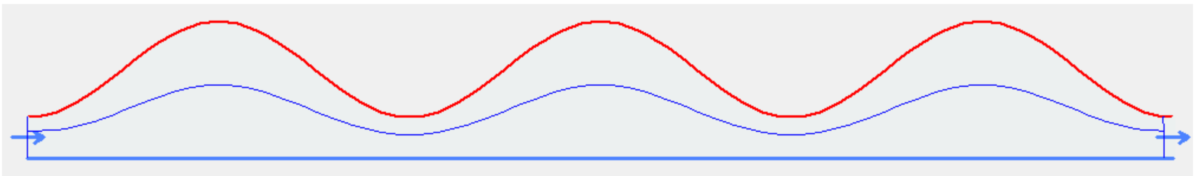

Figure C.14 – Geometric configuration for the implementation in *EasyCFD* (sinusoidal blue line represents the profile option for the inlets).

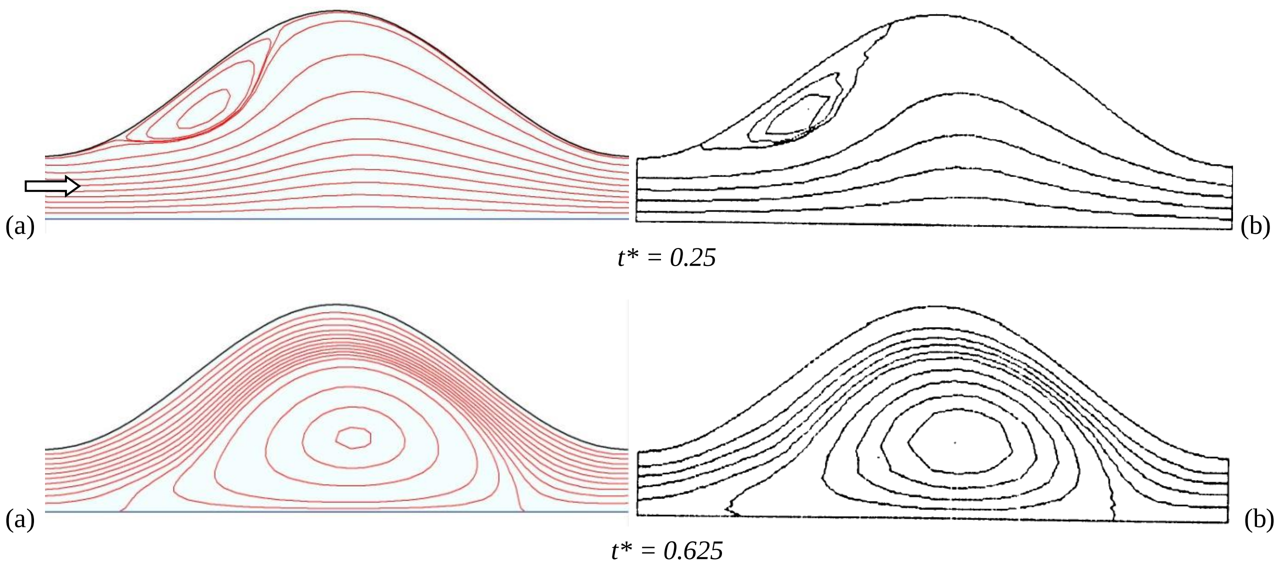

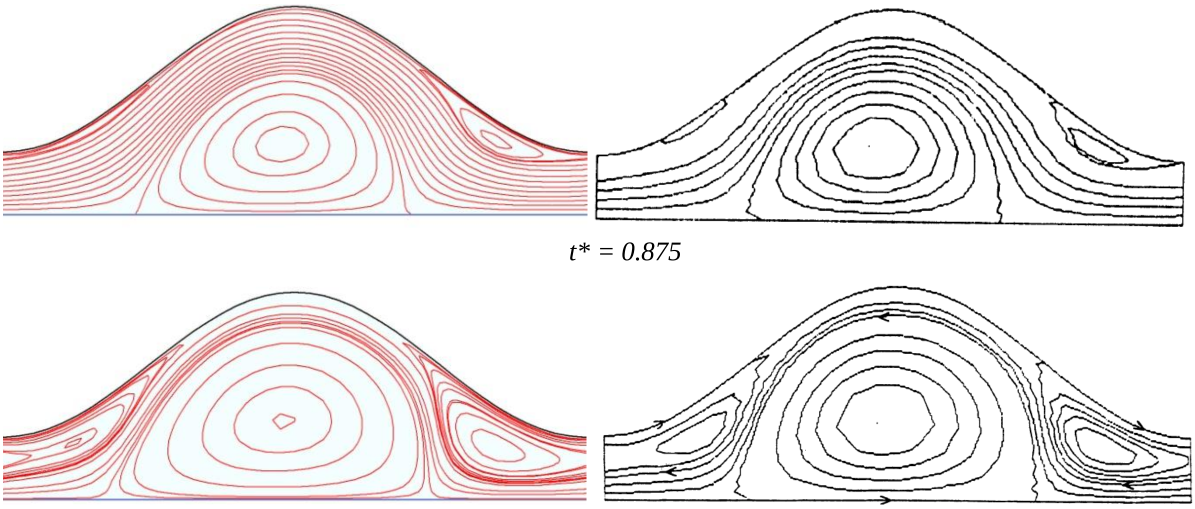

(a) (b)

t = 0.875*

(a) (b)

t = 0.925*

Figure C.15 – Streamlines visualization for different values for the adimensional time. (a): *EasyCFD*; (b): Nishimura e Matsune (1998).

C6 – Drag Coefficient for a sphere

Files: Sphere.def

This problem consists on the determination of drag coefficient of a sphere for a wide range of Reynolds numbers, defined as:

$$Re_D = \frac{\rho V_\infty D}{\mu}$$

where D is the sphere diameter. The drag coefficient is:

$$C_D = \frac{F_x}{0.5\,\rho V_\infty^2 A}$$

where A if the frontal area and F_x is the total force along the streamwise direction. The flow is laminar up to $Re = 3.7E5$, approximately. Flow prediction around the transition regime is particularly difficult due to the large separation region, large scale vortex shedding, etc. Several studies were devoted to this subject, such as, for example, Constantinescua and Squires, 2004.

The present simulations were carried out using the domain presented in Figure C.16. Note that, due to the software limitations, the flow was considered as axisymmetric, though in reality, despite the axisymmetric geometry and boundary conditions, the alternate vortex shedding breaks the symmetry. Due to its tridimensional intrinsic character, this type if phenomena cannot, for the present case, be predicted with EasyCFD.

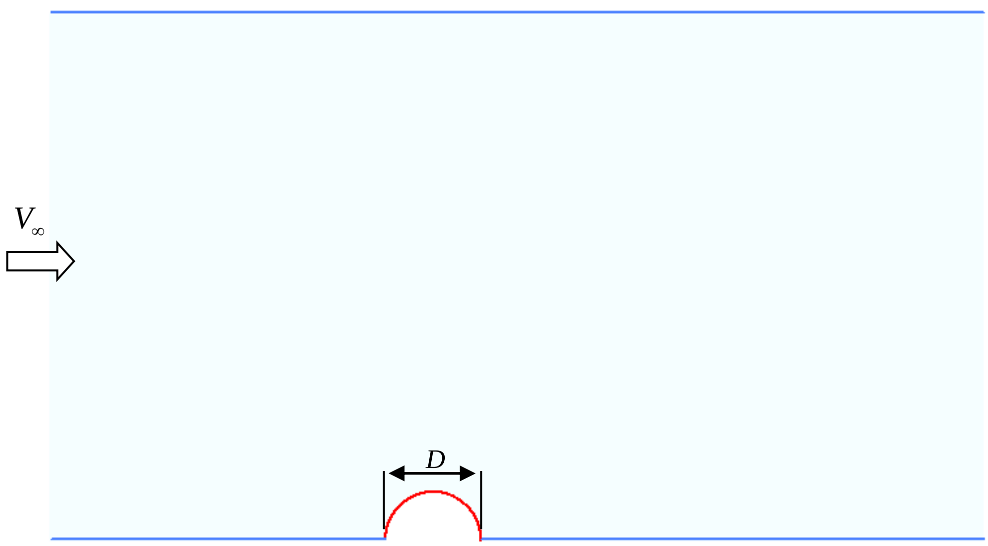

Figure C.16 – Problem definition for the flow around a sphere.

For the turbulent region, both the k-ε and the *SST* k-ω turbulence models were employed. The supplied file *Sphere.def* can be used to solve this problem. The results hereafter presented were computed using the multigrid capability, after doubling twice the unstructured mesh size, from the initial 2063 nodes, up to 8252 nodes and, finally, 33008 nodes (cf. section B1.4.5).

The obtained results are presented in Figure C.17. One may see that results in the laminar region agree very well with experimental data. The turbulent region is not so well predicted, certainly due to the limitations in the turbulence models. The reader is suggested to check for dependency of results with mesh clustering near the sphere, namely with the y^+ values, for the turbulent region.

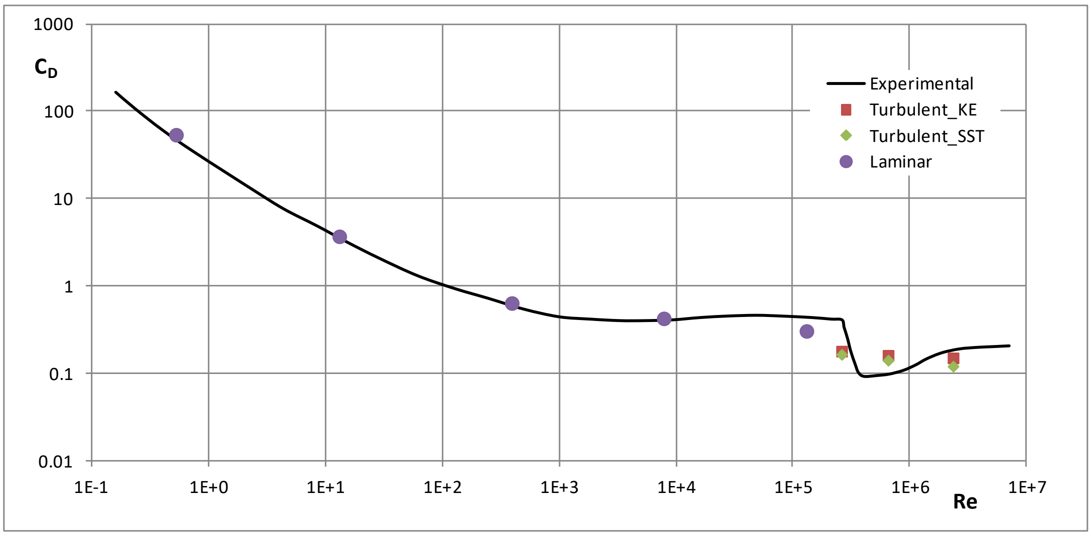

Figure C.17 – Drag coefficient versus Reynolds number, for the flow around a sphere.

C7 – Lift Coefficient for the NACA 2412 Airfoil

Files: Naca2412_NST.dat

This problem consists on the calculation of the lift coefficient for the turbulent flow around a NACA 2412 airfoil. The airfoil profile is given by a point data file, which is imported into **EasyCFD** (cf. section B1.2.8). The lift coefficient C_l is defined as:

$$C_l = \frac{F_z}{0.5\,\rho V_\infty^2 A}$$

where F_z is the total vertical force acting on the profile, V_∞ is the incident wind speed, A is the planform airfoil area (Figure C.18) and ρ is the fluid density. The problem is governed by the flow Reynolds number (assuming that compressible effects are negligible) and by the incidence angle θ.

Calculations were done for $Re = 3.2 \times 10^6$. The results presented in Figure C.19 were obtained with an ustructured mesh of about 20000 nodes. Experimental data was published by Anderson (1989). The agreement is quite reasonable up to the stall region, after which the predictions underestimate the lift coefficient. It must be emphasised that drag and lift values are quite dependent on mesh resolution, so that further calculations should be done with higher resolution meshes. The stall region, which occurs for the present case for angles above 16º is very demanding for turbulence models. It is recognized that most likely the Reynolds average approach, such the one followed by most commercial codes, is not enough for the prediction of such flows.

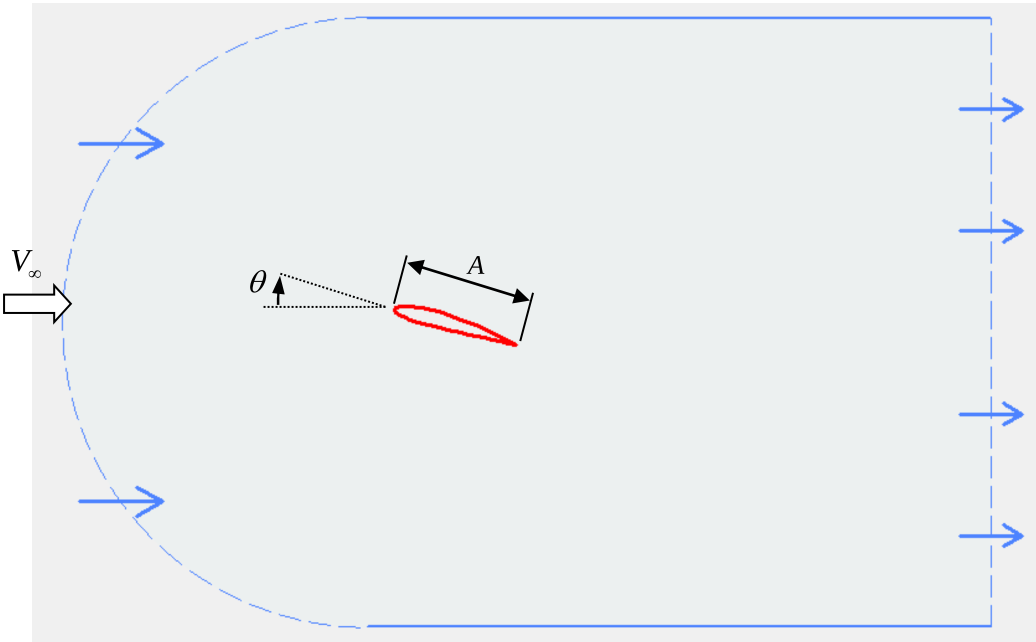

Figure C.18 – Problem definition.

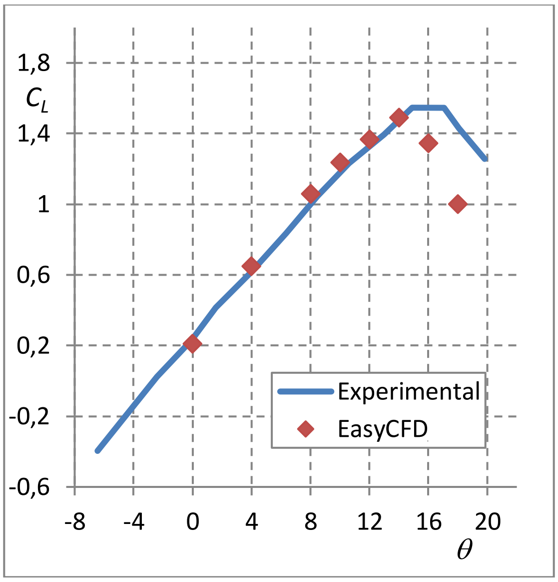

Figure C.19 – Lift coefficient as function of the incidence angle..

The validation cases here presented are, purposely, a starting point for other studies that may contemplate the influence of grid characteristics, advection schemes, inlet conditions for turbulence, etc. Wishing you a good work!!